SCIENTIFIC REPORTS

OPEN

Local stress and pressure in an inhomogeneous system of spherical active Brownian particles

Received: 22 August 2018
Accepted: 15 April 2019
Published online: 29 April 2019

Shibananda Das, Gerhard Gompper & Roland G. Winkler

The stress of a fluid on a confining wall is given by the mechanical wall forces, independent of the nature of the fluid being passive or active. At thermal equilibrium, an equation of state exists and stress is likewise obtained from intrinsic bulk properties; even more, stress can be calculated locally. Comparable local descriptions for active systems require a particular consideration of active forces. Here, we derive expressions for the stress exerted on a local volume of a systems of spherical active Brownian particles (ABPs). Using the virial theorem, we obtain two identical stress expressions, a stress due to momentum flux across a hypothetical plane, and a bulk stress inside of the local volume. In the first case, we obtain an active contribution to momentum transport in analogy to momentum transport in an underdamped passive system, and we introduce an active momentum. In the second case, a generally valid expression for the swim stress is derived. By simulations, we demonstrate that the local bulk stress is identical to the wall stress of a confined system for both, non-interacting ABPs as well as ABPs with excluded-volume interactions. This underlines the existence of an equation of state for a system of spherical ABPs. Most importantly, our calculations demonstrated that active stress is not a wall (boundary) effect, but is caused by momentum transport. We demonstrate that the derived stress expression permits the calculation of the local stress in inhomogeneous systems of ABPs.

The agents of active matter perpetually convert internal energy or energy from the environment into systematic translational motion and are, thus, usually far from thermal equilibrium[1–5]. Their motility gives rise to remarkable phenomena such as collective motion, activity-induced phase transitions[5–17], or wall accumulation[18–21]. Activity is associated with the generation of active stresses, which are responsible for the persistent nonequilibrium state of a system[22–24]. Such stresses are particularly interesting, since there is no equilibrium counterpart and thus, they usually cannot be described by equilibrium thermodynamics. An expression for the active pressure in systems of active Brownian particles (ABPs), based on a generalization of the virial including the active force, has been introduced recently[22,23]. Subsequently, expressions for the active pressure have been derived in various ways for both, the overdamped dynamics of ABPs[25–29] as well as in presence of inertia[30,31].

Mechanical stress/pressure as force per area can be defined even far from equilibrium. The fundamental question is then, how this mechanical pressure is related to nonequilibrium thermodynamics. As a step toward such a relation, the existence of an equation of state for systems of ABPs has been addressed[24,28,32]. Various simulation and theoretical studies confirm that indeed such a relation, including the active pressure, exists for spherical ABPs[22–25,32–34]. However, for (anisotropic) active particles which experience a torque, pressure is in general not a state function anymore[28,35].

A pressure equation of state implies equivalence of wall and local pressure at any point inside the homogeneous relevant volume. Exactly this identity has been questioned in ref.[27]. Typically, confined or periodic systems are considered and relations between wall forces, hence the wall pressure, and virial, including the active-force virial, are determined[22,23,25,28], but no local (bulk) pressure is calculated. Aside from ref.[27], local pressure and the existence of an equation of state has been addressed in ref.[36].

In this article, we derive an instantaneous expression for the local stress (pressure) in a system of spherical active Brownian particles using the virial approach. Thereby, we follow the strategy of ref.[37] for passive systems. A volume ΔV within a larger volume V is considered and an expression is derived for the pressure inside ΔV. Considering the equations of motions of the ABPs inside the volume ΔV, including inertia, we obtain the

Theoretical Soft Matter and Biophysics, Institute of Complex Systems and Institute for Advanced Simulation, Forschungszentrum Jülich, 52425, Jülich, Germany. Correspondence and requests for materials should be addressed to R.G.W. (email: r.winkler@fz-juelich.de)

well-known virial expressions for the pressure of a passive system. In addition, however, we find contributions by activity. On the one hand, we obtain a virial expression for the active stress (swim stress) of particles inside ΔV, which differs from the swim stress discussed so far, and, on the other hand, we find an original momentum-flux contribution of APBs to stress, which we denote as active momentum. The notation rests upon the similarity to the classical linear momentum of a passive particle. It is precisely this term, which distinguishes our studies from those of ref.[27]. In general, we agree with the arguments presented in ref.[27], however, the momentum flux across a plane in the system, similar to the momentum flux by inertia, yields an extra contribution to the local stress which is not considered in ref.[27]. In fact, in ref.[36] an "active impulse, defined as the mean momentum a particle will receive on average from the substrate in the future", is introduce, resembling our instantaneous active momentum, but the meaning is different. By computer simulations of non-interacting ABPs and ABPs interacting by a Lennard-Jones potential, we demonstrate that the derived expressions for the wall and bulk stress are identical. This highlights the existence of a pressure equation state for spherical ABP systems[22,24,36]. Moreover, it opens up the possibility to calculate stresses locally, even in inhomogeneous systems, which we confirm by calculating the local stress in a phase separated system.

Stress in Active Systems

Model. We consider a system of N ABPs of diameter σ in a three-dimensional volume V. Their equations of motion, including the inertia contribution, are given by

$$m\dot{\boldsymbol{r}}_i + \gamma\dot{\boldsymbol{r}}_i(t) = \gamma v_0 \boldsymbol{e}_i(t) + \boldsymbol{F}_i(t) + \boldsymbol{\Gamma}_i(t), \tag{1}$$

where $\boldsymbol{r}_i$, $\dot{\boldsymbol{r}}_i$, and $\boldsymbol{F}_i$ ($i = 1, \ldots, N$) denote the particle positions, velocities, and forces, respectively, m is the mass, γ the translational friction coefficient, and $\boldsymbol{\Gamma}_i$ are Gaussian white-noise random forces, with the moments

$$\langle \boldsymbol{\Gamma}_i(t)\rangle = 0, \quad \left\langle \Gamma_{i\alpha}(t)\Gamma_{j\beta}(t')\right\rangle = 2\gamma k_B T\delta_{\alpha\beta}\delta_{ij}\delta(t - t'). \tag{2}$$

Here, T denotes the temperature, k_B the Boltzmann constant, and $\alpha, \beta \in \{x, y, z\}$ the Cartesian coordinate directions. A particle i is propelled with constant velocity v_0 along its orientation vector $\boldsymbol{e}_i$. The latter changes in a diffusive manner according to

$$\dot{\boldsymbol{e}}_i(t) = \boldsymbol{\eta}_i(t) \times \boldsymbol{e}_i(t) - 2D_R\boldsymbol{e}_i \tag{3}$$

within the Ito interpretation of the multiplicative noise process[38]; $\boldsymbol{\eta}_i$ is a Gaussian and Markovian stochastic process, with the moments

$$\langle \eta_{i\alpha}(t)\rangle = 0, \quad \langle \eta_{i\alpha}(t)\eta_{j\beta}(t')\rangle = \gamma_R\delta_{\alpha\beta}\delta_{ij}\delta(t - t'). \tag{4}$$

The damping factor γ_R is related to the rotational diffusion coefficient, D_R, via $\gamma_R = 2D_R$. Alternatively, the velocity equation of motion of an active Ornstein-Uhlenbeck particle can be considered[39,40], where aside from the orientation also the magnitude of the propulsion velocity is changing. In any case, the correlation function for the active velocity $\boldsymbol{v}_i^{(a)} = v_0\boldsymbol{e}_i$ is[25,39]

$$\langle \boldsymbol{v}_i^{(a)}(t) \cdot \boldsymbol{v}_i^{(a)}(0)\rangle = v_0^2\langle \boldsymbol{e}_i(t) \cdot \boldsymbol{e}_i(0)\rangle = v_0^2 e^{-\gamma_R t}. \tag{5}$$

The forces $\boldsymbol{F}_i$ include contributions from (short-range) interactions with confining walls, $\boldsymbol{F}_i^{(w)}$, as well as possible pair-wise ABP interactions, $\boldsymbol{F}_{ij}$, such that (the prime at the sum indicates that the index $j = i$ is excluded)

$$\boldsymbol{F}_i = \boldsymbol{F}_i^{(w)} + \sum_{j=1}^{N}{}' \boldsymbol{F}_{ij}. \tag{6}$$

Global stress in confined system. We examine now ABPs confined in a rectangle (2D) or cuboid (3D) with walls located at $\pm L_\alpha/2$. The virial expression for the stress follows by multiplying the respective individual Cartesian equations of Eq. (1) by $r_{i\alpha}$, which yields[25,41]

$$\frac{d}{dt}\left[m\langle \dot{r}_{i\alpha}r_{i\alpha}\rangle + \frac{\gamma}{2}\langle r_{i\alpha}^2\rangle\right] = m\langle \dot{r}_{i\alpha}^2\rangle + \gamma\langle v_{i\alpha}^{(a)}r_{i\alpha}\rangle + \langle F_{i\alpha}^{(w)}r_{i\alpha}\rangle + \sum_{j=1}^{N}{}'\left\langle F_{ij\alpha}r_{i\alpha}\right\rangle, \tag{7}$$

where $\langle \ldots \rangle$ denotes either a time or an ensemble average. Due to confinement, the left-hand side of Eq. (7) vanishes. With the definition of an external stress $\sigma_{\alpha\alpha}^{(e)}$ as average total force exerted on a wall,

$$V\sigma_{\alpha\alpha}^{(e)} = \sum_{i=1}^{N}\langle F_{i\alpha}^{(w)}S_{i\alpha}\rangle, \tag{8}$$

where $S_{i\alpha} = \pm L_\alpha/2$ denotes the location of the wall with which particle i interacts, Eq. (7) yields the equivalent internal stress

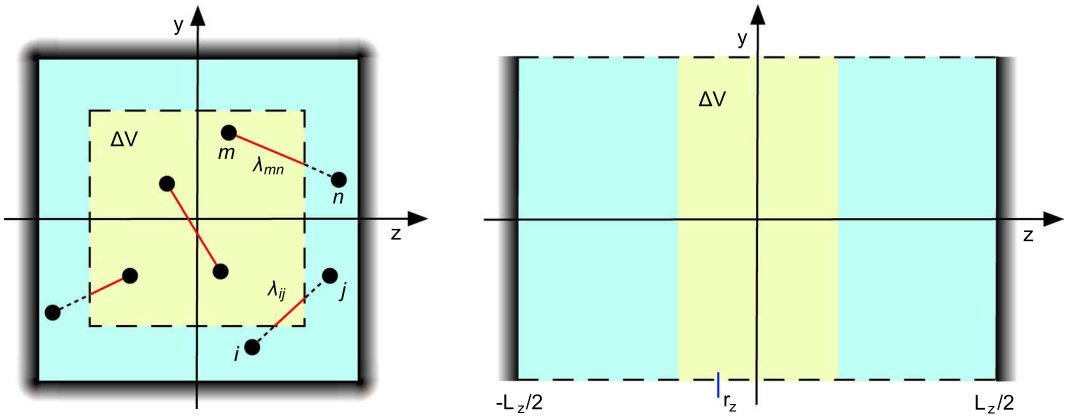

Figure 1. (Left) Schematic of the local subvolume ΔV (yellow) embedded in the bulk of a system confined between walls (light blue). The fraction λ_{ij} of the line joining particle i and j, which lies inside ΔV, is indicated by a solid line. (Right) Schematic of the subvolume ΔV for the calculation of local stress along the z-axis in the simulations. The walls are separated by L_z, and periodic boundaries are applied in the other two directions. The center position of ΔV along the z-axis is denoted by r_z.

$$V\sigma_{\alpha\alpha}^{(i)} = -\sum_{i=1}^{N} m\langle \dot{r}_{i\alpha}^2\rangle - \sum_{i=1}^{N}\gamma\langle v_{i\alpha}^{(a)} r_{i\alpha}\rangle - \sum_{i=1}^{N}\langle F_{i\alpha}^{(w)}(r_{i\alpha} - S_{i\alpha})\rangle - \frac{1}{2}\sum_{i=1}^{N}\sum_{j=1}^{N}{}'\left\langle F_{ij\alpha} r_{ij\alpha}\right\rangle, \tag{9}$$

with $\boldsymbol{r}_{ij} = \boldsymbol{r}_i - \boldsymbol{r}_j$, as sum over all particles of the confined system. Hence, we denote this expression as global (wall) stress. Note that by definition $\sigma_{\alpha\alpha}^{(e)} = \sigma_{\alpha\alpha}^{(i)}$. The contribution with the active force is denoted as swim stress[22,25,42]

$$V\sigma_{\alpha\alpha}^{(s)} = -\sum_{i=1}^{N}\gamma\langle v_{i\alpha}^{(a)} r_{i\alpha}\rangle. \tag{10}$$

The pressure itself follows as $p^{(i,e)} = -(\sum_\alpha \sigma_{\alpha\alpha}^{(i,e)})/3$, where (i, e) refers either to the internal or external pressure or stress. Aside from the wall term with the forces $\boldsymbol{F}_i^{(w)}$, the stress tensor (9) is identical with that derived in ref.[25]. The wall term captures the finite range of the wall force and vanishes in the limit of vanishing wall interaction range.

Local virial and local stress. In order to determine the local stress at the position $\boldsymbol{r}$ within the volume V, we consider a cuboidal subvolume $\Delta V = \Delta L_x \times \Delta L_y \times \Delta L_z$ centered around $\boldsymbol{r}$, with the side lengths ΔL_α (cf. Fig. 1). ABPs inside of ΔV interact with each other as well as ABPs outside. Moreover, ABPs enter and leave ΔV in the course of time. The internal stress follows from the suitable virial expression of ABPs inside of ΔV. To derive the virial expression, as before, we multiply the equations (1) and (3) by $r_{i\alpha}$, an additional factor $\Lambda_{i\alpha}(\boldsymbol{r})$, and sum over all particles. The factor $\Lambda_{i\alpha}$ determines the volume $\Delta V - \Lambda_{i\alpha}(\boldsymbol{r})$ is unity when particle i is within ΔV in the coordinate direction α and zero otherwise[37]. As a result, averaging yields

$$\sum_{i=1}^{N} m\langle \dot{r}_i^2\Lambda_i\rangle + \sum_{i=1}^{N} m\langle \dot{r}_i r_i\dot{\Lambda}_i\rangle + \sum_{i=1}^{N}\langle F_i r_i\Lambda_i\rangle + \sum_{i=1}^{N}\langle \Gamma_i r_i\Lambda_i\rangle + \gamma\sum_{i=1}^{N}\langle v_i^{(a)} r_i\Lambda_i\rangle = 0, \tag{11}$$

$$\sum_{i=1}^{N}\langle e_i\dot{r}_i\Lambda_i\rangle + \sum_{i=1}^{N}\langle e_i r_i\dot{\Lambda}_i\rangle - \gamma_R\sum_{i=1}^{N}\langle e_i r_i\Lambda_i\rangle = 0, \tag{12}$$

with the Ito interpretation of the colored noise process for $\boldsymbol{e}$[25,43], and the relations

$$\frac{d}{dt}\langle \dot{r}_i r_i\Lambda_i\rangle = \langle \ddot{r}_i r_i\Lambda_i\rangle + \langle \dot{r}_i^2\Lambda_i\rangle + \langle \dot{r}_i r_i\dot{\Lambda}_i\rangle, \quad \frac{d}{dt}\langle e_i r_i\Lambda_i\rangle = \langle \dot{e}_i r_i\Lambda_i\rangle + \langle e\dot{r}_i\Lambda_i\rangle + \langle e_i r_i\dot{\Lambda}_i\rangle. \tag{13}$$

Here, and in the following, we often suppress the index α for compactness of the expressions. Due to confinement, the left-hand sides of Eq. (13) vanish. Similarly, the averages $\langle \dot{r}_i r_i\Lambda_i\rangle = \langle r_i^2\dot{\Lambda}_i\rangle = 0$. Inserting the third term of Eq. (12) into Eq. (11), we obtain the virial expression

$$\sum_{i=1}^{N} m\langle \dot{r}_i^2\Lambda_i\rangle + \sum_{i=1}^{N} m\langle \dot{r}_i r_i\dot{\Lambda}_i\rangle + \sum_{i=1}^{N}\langle F_i r_i\Lambda_i\rangle + \frac{\gamma}{\gamma_R}\left[\sum_{i=1}^{N}\langle v_i^{(a)}\dot{r}_i\Lambda_i\rangle + \sum_{i=1}^{N}\langle v_i^{(a)} r_i\dot{\Lambda}_i\rangle\right] = 0. \tag{14}$$

Here, we neglect terms with the averages $\langle \Gamma_i r_i\Lambda_i\rangle$; these averages vanish as long as inertia (cf. Eq. (1)) is taken into account. For an overdamped dynamics, $m = 0$ in Eq. (1), $\langle \Gamma_i r_i\Lambda_i\rangle$ yields the thermal contribution to the stress[25].

For passive systems with $v_0 = 0$, Eq. (14) reduces to the local virial expression in thermal equilibrium presented in ref.[37]. Compared to the global virial[25], additional terms with the derivative of Λ_i, $\dot{\Lambda}_i$, appear due to particles entering and leaving the local volume ΔV. Most remarkably, activity yields a similar contribution as inertia, namely $\gamma \sum_i \langle v_{i\alpha}^{(a)} r_{i\alpha} \dot{\Lambda}_i \rangle / \gamma_R$, compared to $\sum_i \langle m \dot{r}_{i\alpha} r_{i\alpha} \dot{\Lambda}_i \rangle$. This demonstrates that transport of ABPs across a plane yields a contribution to stress similarly to the momentum $\boldsymbol{p}_i^{(m)} = m\dot{\boldsymbol{r}}_i$ of a (passive) particle, in contrast to previous statements[27]. Hence, we can consider

$$\boldsymbol{p}_i^{(a)} = \frac{\gamma}{\gamma_R} \boldsymbol{v}_i^{(a)} \tag{15}$$

as an instantaneous active momentum. Formally, an analogous momentum (impulse) has been introduced in ref.[36] "as momentum the active particle will receive on average from its active force in the future", thus, the meaning is rather different.

Equation (14) includes volume and boundary contributions, where terms with $\dot{\Lambda}_i$ are pure boundary terms. Following the procedure of ref.[37], the following external, $\sigma_{\alpha\alpha}^{(e)}$, and internal, $\sigma_{\alpha\alpha}^{(i)}$, stress tensor components are identified,

$$\begin{aligned} \Delta V \sigma_{\alpha\alpha}^{(e)} = &\sum_{i=1}^{N} m \langle \dot{r}_i r_i \dot{\Lambda}_i \rangle + \frac{\gamma}{\gamma_R} \sum_{i=1}^{N} \langle v_i^{(a)} r_i \dot{\Lambda}_i \rangle + \sum_{i=1}^{N} \sum_{j=1}^{N} \Big\langle (r_i - \lambda_{ij} r_{ij}) F_{ij} \Lambda_i (1 - \Lambda_j) \Big\rangle \\ &- \sum_{i=1}^{N} \sum_{j=1}^{N} \Big\langle \lambda_{ij} r_{ij} F_{ij} (1 - \Lambda_i)(1 - \Lambda_j) \Big\rangle, \end{aligned} \tag{16}$$

$$\Delta V \sigma_{\alpha\alpha}^{(i)} = -\sum_{i=1}^{N} m \langle \dot{r}_i^2 \Lambda_i \rangle - \frac{\gamma}{\gamma_R} \sum_{i=1}^{N} \langle v_i^{(a)} \dot{r}_i \Lambda_i \rangle - \frac{1}{2} \sum_{i=1}^{N} \sum_{j=1}^{N}{}' \Big\langle \lambda_{ij} r_{ij} F_{ij} \Big\rangle. \tag{17}$$

Here, we assume that the volume ΔV is sufficiently far from the surface, and, hence, short-range wall forces do not contribute to the local stress in ΔV. The external stress tensor $\sigma_{\alpha\alpha}^{(e)}$ includes contributions by momentum flux across the boundary, with the active flux $\gamma \sum_{i=1}^{N} \langle v_i^{(a)} r_i \dot{\Lambda}_i \rangle / \gamma_R$, as well as boundary force terms; the third term on the right-hand side of Eq. (16) accounts for stress contributions by forces between particles i inside and j outside of ΔV, and the fourth term for force contributions, when all particles are outside of ΔV, but the connecting line intersects the volume ΔV; λ_{ij} denotes the fraction of the line connecting particle i and j inside of the volume ΔV (cf. Fig. 1)[37]. Note, by suppression of the averages, instantaneous stresses are obtained.

The internal stress tensor $\sigma_{\alpha\alpha}^{(i)}$ (17) includes kinetic contributions from inertia and activity of particles, which are inside the volume of interest, as well as interparticle forces. The interparticle-force term

$$\Delta V \sigma_{\alpha\alpha}^{(if)} = -\frac{1}{2} \sum_{i=1}^{N} \sum_{j=1}^{N}{}' \Big\langle \lambda_{ij} r_{ij} F_{ij} \Big\rangle \tag{18}$$

includes contributions from particles both, inside of ΔV, here $\lambda_{ij} = 1$—this is the standard volume term—, as well as combinations, where a particle is inside and all others, within the finite interaction range, are outside, or both are outside, but their connecting line intersects the volume ΔV, here $\lambda_{ij} < 1$. The latter are boundary terms in analogy to the wall contributions in Eq. (9) of the global system with finite-range wall forces[41].

Remarkably, a new expression for the swim stress is obtained

$$\Delta V \sigma_{\alpha\alpha}^{(s)} = -\frac{\gamma}{\gamma_R} \sum_{i=1}^{N} \langle v_{i\alpha}^{(a)} \dot{r}_{i\alpha} \Lambda_{i\alpha} \rangle, \tag{19}$$

denote as local swim stress in the following, different from the "traditional" swim stress of Eq. (10). Most importantly, the swim stress (10) vanishes in ΔV, and, hence, it is not the adequate expression for the calculation of the local active stress. The vanishing expression (10) in a subvolume lead to the conclusion in ref.[27]. that the local pressure in an ideal active gas is identical with the ideal-gas pressure of passive particles when accounting for the respective local density. As a consequence, it was concluded that the active pressure is a boundary effect, because active forces were not contributing to momentum flux. Our calculations contradict this conclusions. First of all, we find an active flux, Eq. (15), and, secondly, another expression for the local active stress, Eq. (19). The vanishing average of Eq. (10) in ΔV together with Eq. (12) shows that the contribution by the active momentum is the negative of the active virial, i.e.,

$$\sum_{i=1}^{N} \langle p_{i\alpha}^{(a)} r_{i\alpha} \dot{\Lambda}_{i\alpha} \rangle = -\frac{\gamma}{\gamma_R} \sum_{i=1}^{N} \langle v_{i\alpha}^{(a)} \dot{r}_{i\alpha} \Lambda_{i\alpha} \rangle. \tag{20}$$

However, if we extend the volume ΔV to the whole volume V, i.e., $\Lambda_i \equiv 1$, Eq. (3) in the Ito formulation yields $\langle v_{i\alpha}^{(a)} \dot{r}_{i\alpha} \rangle = \gamma_R \langle v_{i\alpha}^{(a)} r_{i\alpha} \rangle$, and Eqs. (9) and (17) become identical. Note that the wall force has then to be taken into account in Eq. (17). Thus, our Eq. (19) is a more general expression for the swim stress, since it applies locally as well as globally.

Global stress of ideal ABP gas. For an ideal gas of ABPs, the interparticle forces are zero, i.e., $\boldsymbol{F}_{ij}=0$, and Eq. (9) becomes

$$V\sigma_{\alpha\alpha}^{(i)} = -Nk_BT - \sum_{i=1}^{N}\gamma\langle v_{i\alpha}^{(a)}r_{i\alpha}\rangle - \sum_{i=1}^{N}\langle F_{i\alpha}^{(w)}(r_{i\alpha}-S_{i\alpha})\rangle, \tag{21}$$

in the overdamped limit, $m=0$. According to refs[24,25], the swim stress (10) can be written as

$$\gamma\langle v_{i\alpha}^{(a)}r_{i\alpha}\rangle = \frac{\gamma}{d\gamma_R}v_0^2 + \frac{1}{\gamma_R}\langle F_{i\alpha}^{(w)}v_{i\alpha}^{(a)}\rangle, \tag{22}$$

where d is the dimension, which leads to the expression

$$V\sigma_{\alpha\alpha}^{(i)} = -Nk_BT - \frac{\gamma}{3\gamma_R}Nv_0^2 - \frac{1}{\gamma_R}\sum_{i=1}^{N}\langle F_{i\alpha}^{(w)}v_{i\alpha}^{(a)}\rangle - \sum_{i=1}^{N}\langle F_{i\alpha}^{(w)}(r_{i\alpha}-L_\alpha)\rangle \tag{23}$$

in 3D. The first term on the right-hand side is the thermal contribution to stress, and the second term the ideal gas swim stress[22,24,25,44,45]

$$\sigma_{\alpha\alpha}^{(id)} = -\frac{\gamma N}{3\gamma_R V}v_0^2. \tag{24}$$

Noteworthy, the wall interaction appears twice in Eq. (23). The term proportional to the active velocity reflects and accounts for wall accumulation, whereas the other term captures finite-range effects of the wall force.

Local stress of ideal ABP gas. For zero interparticle forces, Eq. (17) becomes

$$\Delta V\sigma_{\alpha\alpha}^{(i)} = -\sum_{i=1}^{N}m\langle\dot{r}_{i\alpha}^2\Lambda_{i\alpha}\rangle - \frac{\gamma}{\gamma_R}\sum_{i=1}^{N}\langle v_{i\alpha}^{(a)}\dot{r}_{i\alpha}\Lambda_{i\alpha}\rangle. \tag{25}$$

With the formal solution of Eq. (1),

$$\dot{r}_{i\alpha} = \frac{1}{m}\int_{-\infty}^{t} e^{-\gamma(t-t')/m}[\gamma v_{i\alpha}^{(a)}(t') + F_{i\alpha}(t') + \Gamma_{i\alpha}(t')]dt', \tag{26}$$

we find

$$\langle\dot{r}_{i\alpha}^2\rangle = \frac{k_BT}{m} + \frac{v_0^2}{d(1+m\gamma_R/\gamma)}, \quad \langle v_{i\alpha}^{(a)}\dot{r}_{i\alpha}\rangle = \frac{v_0^2}{d(1+m\gamma_R/\gamma)} \tag{27}$$

in the stationary state. In the evaluation of these expressions, all wall contributions vanish as long as we assume that the volume ΔV is located far enough from a wall such that $e^{-\gamma(t-t_i^{(w)})} \ll 1$, where $t_i^{(w)}$ is the time of the last encounter of an ABP with a wall before entering ΔV. Thus, we obtain

$$\Delta V\sigma_{\alpha\alpha}^{(i)} = -N_{\Delta V}\left(k_BT + \frac{\gamma}{d\gamma_R}v_0^2\right), \tag{28}$$

with $N_{\Delta V}$ the number of ABPs in the volume ΔV. The contributions with the Stokes number $m\gamma_R/\gamma$ cancel, and the result for the overdamped dynamics is obtained, as already discussed in ref.[31]. Evidently, the local stress is independent of the wall force. However, due to wall accumulation, the ABP density is not necessarily homogeneous over the whole volume, in particular, it is reduced in the bulk. Hence, walls can affect the bulk stress and pressure.

For an overdamped and athermal dynamics, Eq. (25) becomes

$$\Delta V\sigma_{\alpha\alpha}^{(i)} = -\frac{\gamma}{\gamma_R}\sum_{i=1}^{N_{\Delta V}}\langle(v_{i\alpha}^{(a)})^2\Lambda_{i\alpha}\rangle = -N_{\Delta V}\frac{\gamma}{3\gamma_R}v_0^2 \tag{29}$$

in 3D by inserting $\dot{r}_{i\alpha} = v_{i\alpha}^{(a)}$ from Eq. (1), Hence, stress is given by the square of the (active) velocity, similar to the case of a passive system.

Evidently, Eqs (23) and (28) become identical in the limit $L_\alpha\to\infty$, i.e., an infinite volume corresponding to the thermodynamic limit in case of a passive system. Then, the local particle density $N_{\Delta V}/\Delta V$ is equal to the density N/V, since finite-size effects and the inhomogeneities by surface accumulation become negligible compared to the overall particle number. However, the equality of the two expressions (23) and (25) applies for all surface separations as long as $(L_\alpha-\Delta L_\alpha)/l_p \gg 1$, where $l_p = v_0/\gamma_R$ is the persistence length of the active motion. The surface forces in Eq. (23) yield additional contributions to the ideal active gas stress. Associated bulk-density variations change the respective values of the local stress (28).

Figure 2 shows simulation results for the local swim stress of non-interacting ABPs in the subvolume ΔV according to Eq. (19) as function of the center position r_z of ΔV, where $L_z=100\sigma$ and $\Delta L_z=0.05L_z$. Activity is characterized by the Péclet number $Pe=v_0/\sigma D_R$, where $Pe=20$ in Fig. 2. In addition, the global wall stress according to Eq. (21) ($k_BT=0$) is presented. Evidently, the local stress is independent of the location of the subvolume

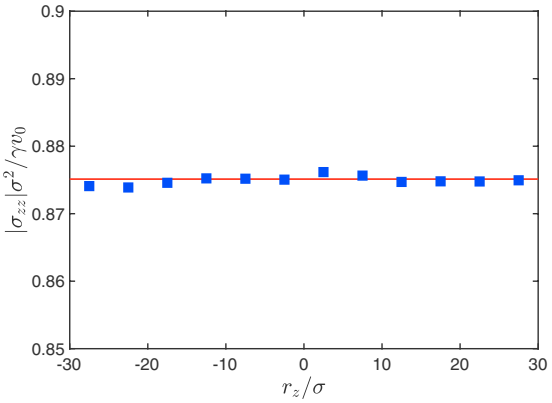

Figure 2. Magnitude of the local stress σ_{zz} according to Eq. (19) in a system of non-interacting ABPs as a function of the center position r_z of the local subvolume ΔV for $Pe = 20$ (blue squares). The side length of the cubic volume V is $L_\alpha = 100\sigma$ and $\Delta L_z = 0.05 L_z$. The solid line (red) indicates the virial stress of the volume V with walls (Eq. (21), $k_B T = 0$).

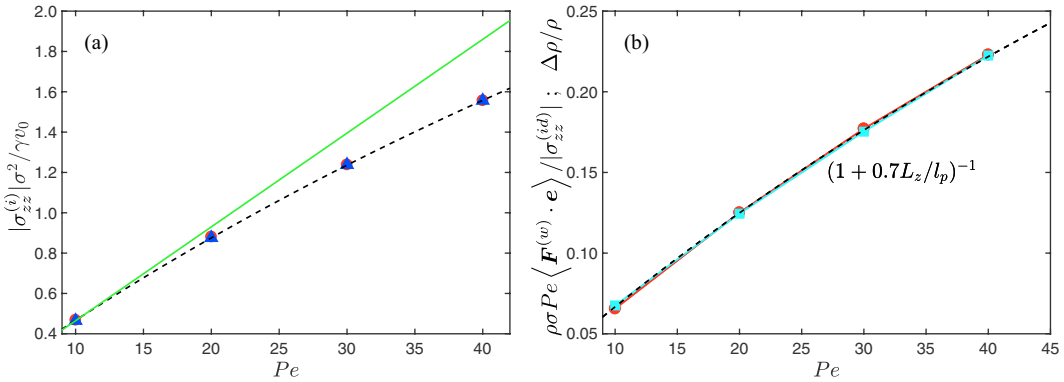

Figure 3. (**a**) Magnitude of the local (blue triangles) and global stress (red bullets) in a system of non-interacting ABPs as a function of the Péclet number Pe. The solid line (green) indicates the ideal swim stress Eq. (24). (**b**) Relative density $\Delta\rho/\rho$ (light blue squares) and the scaled virial of the wall force, $\sum_i \langle F_{i\alpha} v_{i\alpha}^{(a)}\rangle/\gamma_R$, as function of the Péclet number (red bullets). The dashed line represents the fit of Eq. (31). The wall separation is $L_z = 100\sigma$ and $\Delta L_z/L_z = 0.2$. Note that symbols overlap, emphasizing the agreement between the two ways of calculating stress.

ΔV in the bulk of the system and it agrees with the wall stress within 1%. Our results indicate that stress in an active system is not a wall effect. According to Eq. (29), the local stress is proportional to the square of the active velocity of the ABPs within ΔV, similar to the dependence on the kinetic energy in passive systems. Moreover, the simulations confirm the presence of an active momentum flux with the momentum of Eq. (15).

The dependence of the stress on the activity is presented in Fig. 3(a). The local swim stress (19) coincides perfectly with the wall stress (23) ($k_B T = 0$) of the system. The scaled stress

$$\frac{\sigma_{zz}^{(i)}\sigma^2}{\gamma v_0} = -\frac{\rho_{\Delta V}\sigma^3}{6} Pe, \tag{30}$$

where $\rho_{\Delta V} = N_{\Delta V}/\Delta V$ is the bulk density, decreases monotonically with increasing Péclet number, but deviates from the linear dependence of an unconfined (periodic boundary conditions) ideal ABP gas for large Pe[27,46,47]. The stress reduction is a consequence of an enhanced ABP surface accumulation with increasing Pe and, correspondingly, a reduction of the bulk density. Here, we like to emphasize that the stresses calculated via Eqs (8) and (9) perfectly agree with each other.

Figure 3(b) shows the relative density difference $\Delta\rho/\rho = (\rho - \rho_{\Delta V})/\rho$ with respect to the mean density $\rho = N/V$ as function of the Péclet number (squares). The simulation data, with the bulk density $\rho_{\Delta V}$, can well be described by the relation

$$\frac{\Delta\rho}{\rho} = \frac{1}{1 + 0.7 L_z/l_p}, \tag{31}$$

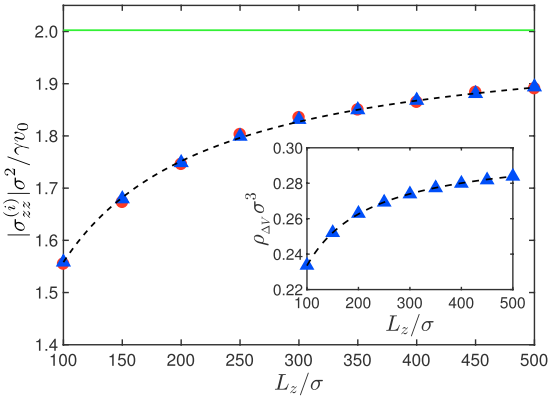

Figure 4. Magnitude of the local (blue triangles) and global stress (red bullets) in a system of non-interacting ABPs as a function of the system size L_z. The solid line (green) indicates the ideal swim stress. The dashed line indicates the stress $\sigma_{zz}^{(i)} = \sigma_{zz}^{(id)}\rho_{\Delta V}/\rho$, where $\Delta\rho/\rho$ is given by Eq. (31). Inset: Variation of the bulk density with wall separation. The dashed line follows from Eq. (31). The Péclet number is $Pe = 40$ and $\Delta L_z/L_z = 0.2$.

which approaches zero in the limits $L_z \to \infty$ and $Pe \to 0$, and the bulk density becomes equal to the average density ρ as for an passive ideal gas. Such a dependence on L_z/l_p has been obtained in ref.[27]. for the fraction of adsorbed ABPs at a wall. However, the numerical factor is somewhat different, we find 0.7 compared to 0.6 in ref.[27]. The difference could be related to the different adopted dimensionalities, $d = 3$ here versus $d = 2$ in ref.[27]. Moreover, Fig. 3(b) shows that the wall virial $\sum_i \langle F_{i\alpha}^{(w)} v_{i\alpha}^{(a)} \rangle / \gamma_R$ (23) divided by the ideal ABP swim stress (24) is identical with the relative density difference $\Delta\rho/\rho$ and, thus, exhibits the same dependence on the Péclet number (the finite-range wall-force contribution is negligible). Of course, this is expected by the equivalence of the stress expressions (21) and (25).

Figure 4 illustrates the dependence of the stress on the wall separation L_z for the Péclet number $Pe = 40$. Again, simulation results for wall and local stress agree very well. With increasing system size, the wall effect decreases and the stress approaches the value of the ideal bulk stress. The relation between the local density and the system size is displayed in the inset of Fig. 4, which is well described by Eq. (31). The dependence of the ideal active gas stress on the Péclet number and system size is solely described by the respective dependence of the density $\rho_{\Delta V}$ on these quantities, since $\sigma_{zz}^{(i)} = \sigma_{zz}^{(id)}\rho_{\Delta V}/\rho$. This is confirmed in Figs 3(a) and 4.

Some of our findings seem to be rather evident as soon as the validity of the Eq. (29) is taken for granted. However, this expression follows from our local stress with the local swim stress (19), and not the stress expression for the system with walls. Specifically, ref.[27] discusses wall-induced effects only. Hence, by our studies we emphasize the existence of a bulk stress and pressure and its identity with the respective wall values.

Interacting ABPs. Simulation results for the local interparticle force (18), local active (19), and global stress of ABP systems with excluded-volume interactions are depicted in Fig. 5(a) as function of the packing fraction ϕ. Again, we obtain excellent agreement between the various stress-tensor contributions calculated both, globally and locally. Consistent with previous studies, the magnitude of the swim stress contribution decreases with increasing density, whereas the magnitude of the interparticle force contribution monotonically increases over the considered concentration range[16,25,48]. Above $\phi \approx 0.4$, the contribution due to interparticle forces dominates the overall stress. Figure 5(b) compares the local swim and interparticle stresses with those in the overall system for various wall distances and concentrations. Remarkably, the local swim stress (bullets) is independent of the wall separation, except for $\phi = 0.25$. In this case, the volume ΔV is not sufficiently far away from the walls, and due to the comparably large persistence length $l_p = 5\sigma$, the ABP velocity is affected by wall interactions (cf. Eq. (26)). The effect vanishes with increasing concentration, since the persistence length decreases due to enhanced particle collisions at higher concentrations. The local swim stress in ΔV (19) can be separated into two contributions by inserting the athermal and overdamped equation of motion (Eq. (1)), namely

$$\sigma_{\alpha\alpha}^{(s)} = \sigma_{\alpha\alpha}^{(id)} - \frac{1}{\gamma_R}\sum_{i=1}^{N}\sum_{j=1}^{N}{}' F_{ij\alpha} v_{i\alpha}^{(a)} \Lambda_{i\alpha}. \tag{32}$$

Hence, the reduction of the relative local swim stress in Fig. 5(a) is a consequence of the correlations between the interparticle forces and the propulsion direction. The effect increases with increasing concentration. We like to emphasize that density variations in the bulk are negligible small for the considered wall separations in Fig. 5(b). In fact, surface accumulation is lower in a system of self-avoiding ABPs compared to an ideal ABP gas. The global swim stress (10) includes, in addition to the terms in Eq. (32), a wall contribution as shown in ref.[25]. It is the latter part, which implies a system-size dependence of the global swim stress (open circles in Fig. 5(b)). The effect gradually vanishes with increasing system size. In contrast, the global interparticle-force stress is independent of system size, which can be expected for a system at constant average density ρ. However, the local interparticle-force stress depends on L_z. Since the total local and global stresses are equal, the system-size dependence of the local interparticle-force stress and that of the global swim stress are equal.

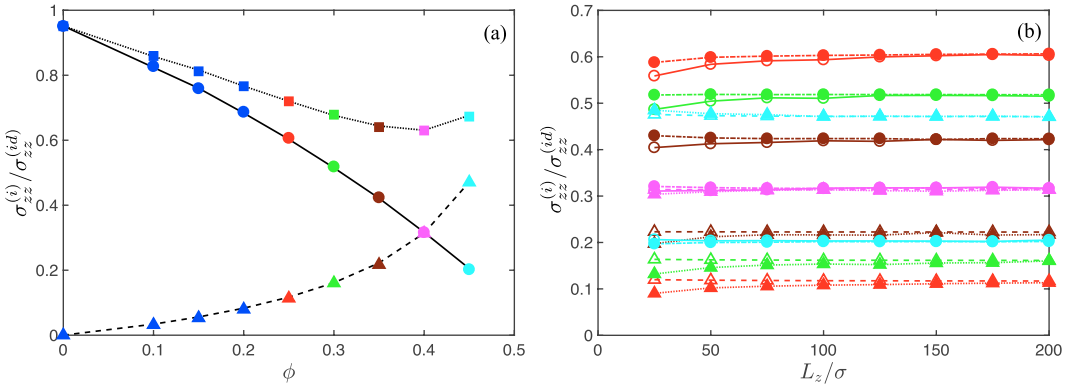

Figure 5. (**a**) Relative local stress $\sigma_{zz}^{(i)}$ with respect to the active ideal gas stress $\sigma_{zz}^{(id)}$ in a system of ABPs with excluded-volume interactions (dotted), the local swim stress (19) (solid), and the contribution by interparticle forces (18) (dashed) as a function of the ABP packing fraction ϕ. The colors refer to systems, where the system-size dependence of the various stress contributions is analyzed (see (**b**)). (**b**) Swim stress (bullets) and interparticle-force stress (triangles) calculated locally (17) (solid) and for the total system including walls (9) (open symbols) as a function of the wall separation L_z for the concentrations $\phi = 0.25$, 0.3, 0.35, 0.4, and 0.45. The color code is the same as in (**a**). Note that the density-dependence changes nonmonotonically. The Péclet number is $Pe = 10$, the wall separation $L_z = 200\sigma$, and the width $\Delta L_z/L_z = 0.2$. The lines are guides for the eye.

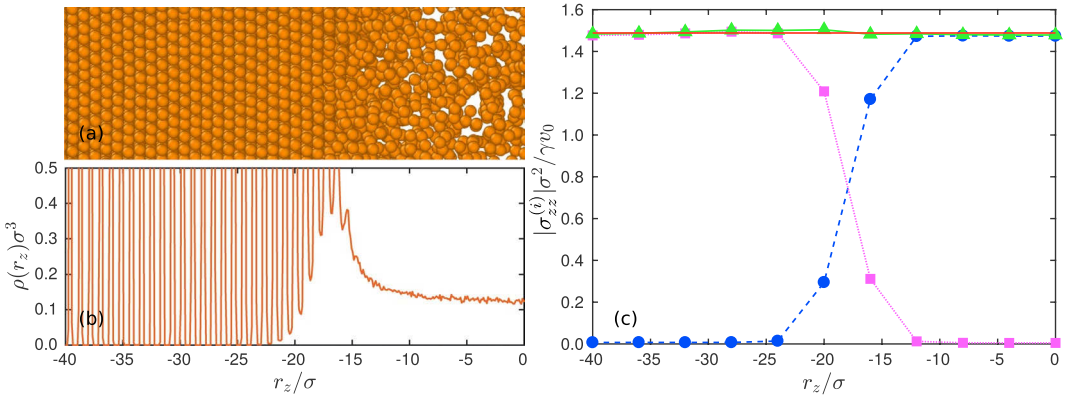

Figure 6. Local (normal) stress in an inhomogeneous ABP system confined between walls. (**a**) Snapshot of a section of the system illustrating the crystalline-like layers adjacent to a wall (left) and the fluid phase in the center (right). (**b**) ABP-density distribution. Due to the pronounced layering adjacent to a wall, the density peaks are narrow and large, exceeding the y-scale by far. (**c**) Contributions of the local swim stress (19) (blue bullets) and the interparticle force stress (18) (magenta squares) to the overall stress (green triangles). The solid red line indicates the global stress calculated via Eq. (9). The size of system is $L_x = L_y = 25\sigma$, $L_z = 100\sigma$, and the width of the local volume $\Delta L_z = 4\sigma$.

Figure 5(b) clearly reveals differences between the global swim (Eq. (9)) and local swim stress (Eq. (17)), specifically for finite system sizes. However, in the thermodynamic limit of infinitely large systems, the two definitions yield identical results. The total stress in a volume V (global) or ΔV (local) is not affected by the difference, since other contributions by interparticle forces yield identical differences and, hence, compensate for the disparity in the swim stresses.

Local stress in inhomogeneous systems of ABPs. The stress in phase-separated, inhomogeneous ABP systems has been calculated before by various methods[49,50]. The calculation of the global stress in ref.[49] is performed with a particle-based model (ABPs) in a system with periodic boundary conditions. However, no stress normal to the interface has been obtained. In ref.[50], a continuum description based on a generalization of the Cahn-Hilliard equation is applied. Here, we illustrate the suitability of our particle-based expression for the calculation of local stresses for a phase-separated system of ABPs confined between two walls. The same geometry is considered as before, but with the dimensions $L_x = L_y = 25\sigma$. The Péclet number $Pe = 80$ is sufficiently large to yield phase separation into crystalline-like layers adjacent to walls and a fluid phase in the center, as is displayed in Fig. 6(a,b). In order to calculate the local stress, we consider local volumes of width $\Delta L_z = 4\sigma$, i.e., we average over four crystalline layers. As shown in Fig. 6(c), the stress normal to the walls and the interface (z direction) is constant over the whole system. Moreover, the local stress agrees with the stress exerted on the wall. In the various

regimes, stress is dominated either by the swim stress (Eq. (19)) (central fluid part) or the force contribution to stress (Eq. (18)) (crystalline wall part). Specifically in the crossover regime, where both stresses contribute, the local stress is equal to the global stress (wall stress). This result confirms that the derived expression is suitable for calculating local stress even in inhomogeneous systems.

Summary and Conclusions

We have derived expressions for the stress (pressure) of a system of confined active Brownian particles, specifically, generally valid expressions for the local stress in a subvolume $\Delta V(\boldsymbol{r})$ centered around a point $\boldsymbol{r}$. In addition to previously derived contributions to the stress of active systems confined between walls[25], the contribution of the finite-range surface interaction is taken into account in the calculation of the global stress. For the stress in a local volume (ΔV), we find two expressions by following the strategy of ref.[37]. On the one hand, stress is given by momentum transfer across a hypothetical plane, including force as well as kinetic (momentum) contributions. Here, we find a motility contribution by introducing an active momentum in analogy to the kinetic momentum of a particle of mass m. On the other hand, we identify a virial expression for the active stress (local swim stress) of particles inside of ΔV, different from the known swim stress[22,25,42]. In fact, in ref.[36] a formally similar expression has been defined, however, with an active impulse of very different meaning. Computer simulations show that our obtained local stress expression agrees quantitatively with the corresponding global stress expression of an ABP system confined between walls for both, non-interacting ABPs as well as ABPs interacting via a Lennard-Jones potential. This underlines the existence of an equation of state for a system of spherical ABPs.

Our results reach beyond previous considerations and discussions on the stress in active systems. Initially, swim pressure has been introduce via Clausius' virial[51], taking active forces into account[22,23]. Based on the equations of motion of ABPs for an infinite system, the swim pressure of an ideal active gas has then been proposed[22]. Subsequently, derivations of active pressure expressions have been presented for ABPs confined between walls[25–27] or in periodic systems[25,27]. Alternatively, pressure expressions have been determined via the Fokker-Planck equation of an ABP system[28], or the equations of motion for the density field[36]. A derivation of an expression for a local pressure has be attempted in ref.[27], with the conclusion that a local pressures exists, but the bulk value differs from the mechanical pressure exerted on confining walls. In case of an ideal gas of ABPs, the bulk pressure would be given by $\rho(\boldsymbol{r})k_BT$, with the position dependent density $\rho(\boldsymbol{r})$ and, hence, would vanish in an athermal system. Hence, active pressure is considered as a boundary effect[27]. In contrast, the present calculations provide a general expression for the local stress and pressure and thus, mark a substantial advancement. The derived local stress/pressure expressions are more general and reduce to the known expressions in the limit of the local volume being equal to the overall volume. This is emphasized by the fact that the local swim stress (19) is finite, while the "traditional" swim stress (10) vanishes in ΔV. Most importantly, our calculations demonstrated that active stress/pressure is not a wall (boundary) effect, as stated in ref.[27], but is caused by active momentum transport in analogy to momentum transfer in a passive system. Hence, our results allow us to resolve apparent contradictions in the interpretation of local stress and consequently in the existence of equations of state in active systems.

As we demonstrated, local stress or pressure can be calculated in inhomogeneous ABP systems. Extensions to local shear stresses are straightforward and, thus, surface tensions of active systems can be determined.

Methods

We perform simulations in three dimensions considering the overdamped Eq. (1), $m=0$, without thermal fluctuations. The translational equations of motion (1) are solved via the Ermak-McCammon algorithm[52]. The equations of motion (3) for the orientation vectors are solved using the scheme described in ref.[25].

Pair-wise interparticle interactions are taken into account by the repulsive Lennard-Jones potential

$$U_{LJ}=\begin{cases}\varepsilon\left[\left(\frac{\sigma}{r_{ij}}\right)^{12}-\left(\frac{\sigma}{r_{ij}}\right)^{6}+\frac{1}{4}\right], & r_{ij}\le \sqrt[6]{2}\sigma\\ 0, & r_{ij}>\sqrt[6]{2}\sigma\end{cases}, \tag{33}$$

where $r_{ij}=|\boldsymbol{r}_{ij}|$ and the interaction strength is set to $\varepsilon/k_BT=Pe$; Pe is the Péclet number defined as

$$Pe=\frac{v_0}{\sigma D_R}. \tag{34}$$

This yields the same particle overlap independent of the Péclet number[53]. The ABPs are confined between two walls parallel to the xy-plane of the Cartesian reference frame located at $S_{iz}=\pm L_z/2$ (cf. Fig. 1). Parallel to the walls, periodic boundary conditions are applied. The purely repulsive ABP-wall interaction is described by the Lennard-Jones potential of Eq. (33) with r_{ij} replaced by z_i-S_{iz}.

We determine the stress σ_{zz} along the z-axis in two ways. Firstly, we calculate the global stress of the whole system according to Eq. (9) ($m=0$). Secondly, the local stress in a volume ΔV is calculated via Eq. (17). Thereby, the box dimension L_z normal to the walls is chosen such that it is significantly larger than the persistence length $l_p=v_0/2D_R=Pe\sigma/2$ of an ABP, in particular, we consider wall separations $L_z\geqslant 5l_p$. The volume ΔV of width ΔL_z is located in the bulk of the system along the z-axis (cf. Fig. 1). If not indicated otherwise, the dimensions of the volume V are $L_x=L_y=40\sigma$, $L_z=100\sigma$, and $\Delta L_z=0.2L_z$. In Fig. 1, r_z denotes the position of the center of the slit within the interval $L_z/2<r_z<L_z/2$. The number density of ABPs in V is $\rho\sigma^3=0.3$. We perform at least three independent simulations runs of 2×10^7 time steps each, with the time step $dt=10^{-3}\sigma/v_0$. Thus, every presented data point is averaged over approximately 10^3 independent configurations.

References

1. Ramaswamy, S. The mechanics and statistics of active matter. *Annu. Rev. Cond. Mat. Phys.* **1**, 323, https://doi.org/10.1146/annurev-conmatphys-070909-104101 (2010).
2. Cates, M. E. & MacKintosh, F. C. Active soft matter. *Soft Matter* **7**, 3050, https://doi.org/10.1039/C1SM90014E (2011).
3. Marchetti, M. C. *et al.* Hydrodynamics of soft active matter. *Rev. Mod. Phys.* **85**, 1143, https://doi.org/10.1103/RevModPhys.85.1143 (2013).
4. Elgeti, J., Winkler, R. G. & Gompper, G. Physics of microswimmers-single particle motion and collective behavior: a review. *Rep. Prog. Phys.* **78**, 056601, https://doi.org/10.1088/0034-4885/78/5/056601 (2015).
5. Bechinger, C. *et al.* Active particles in complex and crowded environments. *Rev. Mod. Phys.* **88**, 045006, https://doi.org/10.1103/RevModPhys.88.045006 (2016).
6. Fily, Y. & Marchetti, M. C. Athermal phase separation of self-propelled particles with no alignment. *Phys. Rev. Lett.* **108**, 235702, https://doi.org/10.1103/PhysRevLett.108.235702 (2012).
7. Theurkauff, I., Cottin-Bizonne, C., Palacci, J., Ybert, C. & Bocquet, L. Dynamic clustering in active colloidal suspensions with chemical signaling. *Phys. Rev. Lett.* **108**, 268303, https://doi.org/10.1103/PhysRevLett.108.268303 (2012).
8. Buttinoni, I. *et al.* Dynamical clustering and phase separation in suspensions of self-propelled colloidal particles. *Phys. Rev. Lett.* **110**, 238301, https://doi.org/10.1103/PhysRevLett.110.238301 (2013).
9. Redner, G. S., Hagan, M. F. & Baskaran, A. Structure and dynamics of a phase-separating active colloidal fluid. *Phys. Rev. Lett.* **110**, 055701, https://doi.org/10.1103/PhysRevLett.110.055701 (2013).
10. Bialké, J., Speck, T. & Löwen, H. Crystallization in a dense suspension of self-propelled particles. *Phys. Rev. Lett.* **108**, 168301, https://doi.org/10.1103/PhysRevLett.108.168301 (2012).
11. Wittkowski, R. *et al.* Scalar ϕ^4 field theory for active-particle phase separation field theory for active-particle phase separation. *Nat. Commun.* **5**, 4351 (2014).
12. Cates, M. E. & Tailleur, J. Motility-induced phase separation. *Annu. Rev. Condens. Matter Phys.* **6**, 219, https://doi.org/10.1146/annurev-conmatphys-031214-014710 (2015).
13. Wysocki, A., Winkler, R. G. & Gompper, G. Cooperative motion of active Brownian spheres in three-dimensional dense suspensions. *EPL* **105**, 48004, https://doi.org/10.1209/0295-5075/105/48004 (2014).
14. Stenhammar, J., Marenduzzo, D., Allen, R. J. & Cates, M. E. Phase behaviour of active Brownian particles: the role of dimensionality. *Soft Matter* **10**, 1489, https://doi.org/10.1039/C3SM52813H (2014).
15. Wysocki, A., Winkler, R. G. & Gompper, G. Propagating interfaces in mixtures of active and passive Brownian particles. *New J. Phys.* **18**, 123030, https://doi.org/10.1088/1367-2630/aa529d (2016).
16. Marchetti, M. C., Fily, Y., Henkes, S., Patch, A. & Yllanes, D. Minimal model of active colloids highlights the role of mechanical interactions in controlling the emergent behavior of active matter. *Curr. Opin. Colloid Interface Sci.* **21**, 34, https://doi.org/10.1016/j.cocis.2016.01.003 (2016).
17. Theers, M., Westphal, E., Qi, K., Winkler, R. G. & Gompper, G. Clustering of microswimmers: interplay of shape and hydrodynamics. *Soft Matter* **14**, 8590, https://doi.org/10.1039/C8SM01390J (2018).
18. Berke, A. P., Turner, L., Berg, H. C. & Lauga, E. Hydrodynamic attraction of swimming microorganisms by surfaces. *Phys. Rev. Lett.* **101**, 038102, https://doi.org/10.1103/PhysRevLett.101.038102 (2008).
19. Lee, C. F. Active particles under confinement: aggregation at the wall and gradient formation inside a channel. *New J. Phys.* **15**, 055007, https://doi.org/10.1088/1367-2630/15/5/055007 (2013).
20. Elgeti, J. & Gompper, G. Wall accumulation of self-propelled spheres. *EPL* **101**, 48003 (2013).
21. Fily, Y., Baskaran, A. & Hagan, M. F. Dynamics of self-propelled particles under strong confinement. *Soft Matter* **10**, 5609, https://doi.org/10.1039/C4SM00975D (2014).
22. Takatori, S. C., Yan, W. & Brady, J. F. Swim pressure: Stress generation in active matter. *Phys. Rev. Lett.* **113**, 028103, https://doi.org/10.1103/PhysRevLett.113.028103 (2014).
23. Yang, X., Manning, M. L. & Marchetti, M. C. Aggregation and segregation of confined active particles. *Soft Matter* **10**, 6477, https://doi.org/10.1039/C4SM00927D (2014).
24. Solon, A. P. *et al.* Pressure and phase equilibria in interacting active Brownian spheres. *Phys. Rev. Lett.* **114**, 198301, https://doi.org/10.1103/PhysRevLett.114.198301 (2015).
25. Winkler, R. G., Wysocki, A. & Gompper, G. Virial pressure in systems of spherical active Brownian particles. *Soft Matter* **11**, 6680, https://doi.org/10.1039/C5SM01412C (2015).
26. Falasco, G., Baldovin, F., Kroy, K. & Baiesi, M. Mesoscopic virial equation for nonequilibrium statistical mechanics. *New J. Phys.* **18**, 093043, https://doi.org/10.1088/1367-2630/18/9/093043 (2016).
27. Speck, T. & Jack, R. L. Ideal bulk pressure of active Brownian particles. *Phys. Rev. E* **93**, 062605, https://doi.org/10.1103/PhysRevE.93.062605 (2016).
28. Solon, A. P. *et al.* Pressure is not a state function for generic active fluids. *Nat. Phys.* **11**, 673, https://doi.org/10.1038/nphys3377 (2015).
29. Steffenoni, S., Falasco, G. & Kroy, K. Microscopic derivation of the hydrodynamics of active-Brownian-particle suspensions. *Phys. Rev. E* **95**, 052142, https://doi.org/10.1103/PhysRevE.95.052142 (2017).
30. Joyeux, M. & Bertin, E. Pressure of a gas of underdamped active dumbbells. *Phys. Rev. E* **93**, 032605, https://doi.org/10.1103/PhysRevE.93.032605 (2016).
31. Takatori, S. C. & Brady, J. F. Inertial effects on the stress generation of active fluids. *Phys. Rev. Fluid* **2**, 094305, https://doi.org/10.1103/PhysRevFluids.2.094305 (2017).
32. Ginot, F. *et al.* Nonequilibrium equation of state in suspensions of active colloids. *Phys. Rev. X* **5**, 011004, https://doi.org/10.1103/PhysRevX.5.011004 (2015).
33. Bertin, E. An equation of state for active matter. *Phys.* **8**, 44, https://doi.org/10.1103/Physics.8.44 (2015).
34. Nikola, N. *et al.* Active particles with soft and curved walls: Equation of state, ratchets, and instabilities. *Phys. Rev. Lett.* **117**, 098001, https://doi.org/10.1103/PhysRevLett.117.098001 (2016).
35. Junot, G., Briand, G., Ledesma-Alonso, R. & Dauchot, O. Active versus passive hard disks against a membrane: Mechanical pressure and instability. *Phys. Rev. Lett.* **119**, 028002, https://doi.org/10.1103/PhysRevLett.119.028002 (2017).
36. Fily, Y., Kafri, Y., Solon, A. P., Tailleur, J. & Turner, A. Mechanical pressure and momentum conservation in dry active matter. *J. Phys. A: Math. Theor.* **51**, 044003, https://doi.org/10.1088/1751-8121/aa99b6 (2018).
37. Lion, T. W. & Allen, R. J. Computing the local pressure in molecular dynamics simulations. *J. Phys.: Condens. Matter* **24**, 284133, https://doi.org/10.1088/0953-8984/24/28/284133 (2012).
38. Raible, M. & Engel, A. Langevin equation for the rotation of a magnetic particle. *Appl. Organometal. Chem.* **18**, 536, https://doi.org/10.1002/aoc.757 (2004).
39. Das, S., Gompper, G. & Winkler, R. G. Confined active Brownian particles: theoretical description of propulsion-induced accumulation. *New J. Phys.* **20**, 015001, https://doi.org/10.1088/1367-2630/aa9d4b (2018).
40. Fodor, É. *et al.* How far from equilibrium is active matter? *Phys. Rev. Lett.* **117**, 038103, https://doi.org/10.1103/PhysRevLett.117.038103 (2016).
41. Winkler, R. G. & Hentschke, R. Liquid benzene confined between graphite surfaces. a constant pressure molecular dynamics study. *J. Chem. Phys.* **99**, 5405 (1993).

42. Takatori, S. C. & Brady, J. F. Swim stress, motion, and deformation of active matter: effect of an external field. *Soft Matter* **10**, 9433, https://doi.org/10.1039/C4SM01409J (2014).
43. Risken, H. *The Fokker-Planck Equation*. (Springer, Berlin, 1989).
44. Mallory, S. A., Šarić, A., Valeriani, C. & Cacciuto, A. Anomalous thermomechanical properties of a self-propelled colloidal fluid. *Phys. Rev. E* **89**, 052303, https://doi.org/10.1103/PhysRevE.89.052303 (2014).
45. Smallenburg, F. & Löwen, H. Swim pressure on walls with curves and corners. *Phys. Rev. E* **92**, 032304, https://doi.org/10.1103/PhysRevE.92.032304 (2015).
46. Yan, W. & Brady, J. F. The force on a boundary in active matter. *J. Fluid Mech.* **785**, R1, https://doi.org/10.1017/jfm.2015.621 (2015).
47. Ezhilan, B., Alonso-Matilla, R. & Saintillan, D. On the distribution and swim pressure of run-and-tumble particles in confinement. *J. Fluid Mech.* **781**, R4, https://doi.org/10.1017/jfm.2015.520 (2015).
48. Takatori, S. C. & Brady, J. F. Forces, stresses and the (thermo?) dynamics of active matter. *Curr. Opin. Colloid Interface Sci.* **21**, 24, https://doi.org/10.1016/j.cocis.2015.12.003 (2016).
49. Bialké, J., Siebert, J. T., Löwen, H. & Speck, T. Negative interfacial tension in phase-separated active Brownian particles. *Phys. Rev. Lett.* **115**, 098301, https://doi.org/10.1103/PhysRevLett.115.098301 (2015).
50. Solon, A. P., Stenhammar, J., Cates, M. E., Kafri, Y. & Tailleur, J. Generalized thermodynamics of phase equilibria in scalar active matter. *Phys. Rev. E* **97**, 020602, https://doi.org/10.1103/PhysRevE.97.020602 (2018).
51. Becker, R. *Theory of Heat*. (Springer Verlag, Berlin, 1967).
52. Ermak, D. L. & McCammon, J. Brownian dynamics with hydrodynamic interactions. *J. Chem. Phys.* **69**, 1352, https://doi.org/10.1063/1.436761 (1978).
53. Fily, Y., Henkes, S. & Marchetti, M. C. Freezing and phase separation of self-propelled disks. *Soft Matter* **10**, 2132, https://doi.org/10.1039/C3SM52469H (2014).

Acknowledgements

Financial support by the Deutsche Forschungsgemeinschaft (DFG) within the priority program SPP 1726 "Microswimmers—from Single Particle Motion to Collective Behaviour" is gratefully acknowledged.

Author Contributions

R.G.W. and G.G. conceived the project. R.G.W. and S.D. performed the analytical calculations. S.D. designed the simulation algorithm and performed the simulations. R.G.W., S.D., and G.G. interpreted the data and wrote the paper. All authors discussed the results and commented on the manuscript.

Additional Information

Competing Interests: The authors declare no competing interests.

Publisher's note: Springer Nature remains neutral with regard to jurisdictional claims in published maps and institutional affiliations.